MJFAS
Malaysian Journal of Fundamental and Applied Sciences

RESEARCH ARTICLE

Aluminum Doped Titanium Dioxide Thin Film for Perovskite Electron Transport Layer

Faiz Hashim[a,*], Khamim Ismail[a], Aizuddin Supee[b], Firdaus Omar[a], Zainatul Izzah Ab. Ghani[a], Ain Ajeerah Ramli[a], and Syariffah Nurathirah Syed Yaacob[a]

[a] Department of Physic, Faculty of Science; 81310 UTM Johor Bahru, Johor, Malaysia; [b] Department of Energy Engineering, School of Chemical and Energy Engineering; 81310 UTM Johor Bahru, Johor, Malaysia

Abstract Aluminum (Al) doped titanium dioxide thin film with different Al doping concentration (Al = 0 mol%, 1 mol%, 3 mol%, 5 mol% and 7 mol%) were deposited using solution spin coating technique and the effect of Al concentration on the structural, morphological and optical properties were examine. All samples were annealed at 450°C for 1 hour. XRD revealed that the films exhibits anatase crystal phase at (101) peak orientation. Based on the FESEM and AFM images it is found that, surface morphology of the film was significantly affected with different doping concentration. Al doped titanium dioxide with 3 mol% Al concentration shows the highest transmittance compared to other samples. Consequently, it is shown that different Al doping concentration plays vital roles in producing an optimum Al doped titanium dioxide thin film samples.

Keywords: Titanium Dioxide, Aluminum, Thin Film, Perovskite Solar Cell, Electron Transport Layer.

Introduction

Metal oxide semiconductors (MOS) have attract the interest of experts in the science and technology industry for many years and have been utilised in a number of technologies. High chemical, physical, and thermal stability, high transmittance in the visible region, significant photocatalytic activities, non-toxicity, and a cost-effective production method are a few of the qualities that make this material ideal for thin film applications. [1]–[4]. Titanium dioxide (TiO_2) is recognised as the most adaptable MOS material among others such as In_2O_3, ZnO, and SnO_3 because to its extensive technological applications, including gas sensors [5], photocatalysts [6]–[8], biomedical [9], and solar cell devices [10]–[13].

TiO_2, often referred to as titania, may occur in three distinct structural phases: brookite, rutile, and anatase [14], [15]. Generally, anatase and rutile have tetragonal crystal phase, but brookite has orthorhombic crystal phase, depending on the fabrication conditions and variables [16]. Several technique were adopted to fabricate TiO_2 thin film, for example, pulsed laser deposition[17], sputtering[18], hydrothermal treatment [19] chemical vapour deposition[20], spray pyrolysis [21], dip coating [22] and spin coating [3], [23].

By having high absorption, high chemical and mechanical stability and wide energy bandgap, makes titanium dioxide (TiO_2) a suitable candidate for photovoltaic application [24]. However, the relatively high surface trap state of pure TiO_2 has impeded the development of solar devices [25][26]. Numerous strategies have been implemented to enhance the characteristics of pure TiO<2>, by modifying the composition of pure TiO_2 thin film by injecting dopant material. The characteristic and properties of TiO_2 thin film can be simply control by introduction of dopant materials. Modification of TiO_2 thin film composition with appropriate substitution ion such as Y^{3+} [27], Mg^{2+} [28], Sn^{4+} [29] and Nd^{3+} [30] has been demonstrated by many researchers. It is found that, introduction of dopant materials such as Aluminum (Al), will reduce

***For correspondence:**
faizhashim232@gmail.com

Received: 11 Jan. 2022
Accepted: 31 Oct. 2022

the surface trap state and increased the overall efficiencies of the solar cell by removing the oxygen defect from the TiO_2 lattice [31]. Even though there are many studies had been explored Al doped TiO_2, yet the optimum concentration of Al dopant and the effect of Al doping are still in fact not always clearly understood [8], [31], [32]. As for photovoltaic application, higher light transmittance through the window layer is important in TiO_2 based photovoltaic cells. Bhat *et al*. reported that significant changes in the transmittance of the prepared film with the increase of the of Al dopant percentage [13].

Therefore, in this paper we demonstrate the preparation process of Al doped TiO_2 thin film using solution process spin coating method, and investigate the effect of Al doping on the TiO_2 thin film layers on its surface morphology, structural and optical properties. Al doping concentration is varied from 0.0 mol%, 1.0 mol%, 3.0 mol%, 5.0 mol% and 7.0 mol%. The aim of this study is to produce a superior Al doped TiO_2 thin film samples with high crystallinity and high transmittance that can be used for future solar cell development.

Materials and Methods

Al:TiO_2 thin samples with different Al doping concentration were prepared using a simple and cost-effective spin coating method. Titanium (IV) isopropoxide (TTiP) (Ti[$OCH(CH_3)_2$]$_4$, 97%) (Sigma Aldrich), ethanol 95% (Bendosen), hydrochloric acid (conc. 37%) (RCI Labscan) and deionized water were used as starting materials to produce TiO_2 solution. In general, two different solutions (solution A and solution B) were prepared first at room temperature. For solution A, a mixture of 3 ml of ethanol and 5 ml of deionized water were stirred for 30 minutes, followed by the addition of 0.4 ml HCl at the end of the stirring. Simultaneously, 1 ml of TTiP and 2 ml of ethanol were vigorously stirred for 30 minutes to produce solution B. Then, both solutions A and solution B were mixed together under continuous stirring for 1 hour and then they are kept in dark confinement space for 12 hours ageing process. Al:TiO_2 thin films with different Al doping concentration (Al concentration = 0.0 mol%, 0.5 mol%, 1.0 mol%, 1.5 mol% and 2.0 mol%) were prepared by adding aluminum nitrate ($(AlNO_3)3{\cdot}H_2O$) powder (Sigma Aldrich) to TiO_2 solution prepared earlier. Each solution mixture was mixed thoroughly and homogenous transparent solutions were obtained.

Soda lime glass (SLG) substrates were used as the substrate to hold the deposited Al:TiO_2 thin film samples. First, the glass substrates were cut into a desired size (dimensions: 10mm×10mm×1.3 mm) and cleaned using an ultrasonic cleaner. The prepared Al:TiO_2 solution then was spin coated on top of SLG substrates at a spin speed of 3500 rpm for 60 s. MTI VTC-100 spin coater unit were employed in fabricating Al:TiO_2 thin film samples. After successive coating of Al:TiO_2 layer, the substrates than dried at 150°C for 5 minutes using a hot plate in air ambiance. The process of coating and drying process were repeated for five times for each sample. Finally, the deposited samples were annealed at 450°C in vacuum environment using tube furnace for 60 minutes for the samples recrystallization process. All thin films samples with different aluminum doping concentration were characterized and analyzed thoroughly.

Characterization Process

The structural analysis was performed using X-ray diffraction (XRD) diffractometer (Rigaku SmartLab) with wavelength of Cu Kα (~1.54060Å at 30mA and 40kV) and 2θ ranging from 10° to 80°. The surface roughness of Al:TiO_2 thin film were observed using atomic force microscope (AFM) (SPA300HV AFM probe station) in dynamic force mode at ambient temperature. Field emission scanning electron microscope (FESEM) (Hitachi SU8000 In-line FE-SEM) utilizing 10.0kV accelerating voltage with magnification of x250k were used to observe surface morphology and elemental composition of Al:TiO_2 thin film. The transmittance of Al:TiO_2 thin film were measured using UV-Vis spectrophotometer (Shimadzu UV-3600 Plus) in the wavelength ranging from 300 – 700 nm.

Results and Discussion

Structural Properties

X-ray diffraction pattern shows that all samples are crystalline and all peaks can be assigned to anatase phase of TiO_2 with prominent peak of (101) at 2θ = 25.45°. No other diffraction peaks related to Al dopant were detected, suggesting that Al dopant materials did not develop a significant phase. Based on the XRD pattern, it is found that the diffraction peaks intensities of the samples were intensified slightly and reach highest peak intensity as the dopant concentration increased to 3.0 mol%, which indicates that high crystalline thin film is obtained. As the Al doping concentration increased, the TiO_2 diffraction peaks became smaller and weaker due to high structural disorder caused by the substitution of different ionic radius of Al^{3+} and Ti^{4+} [33].

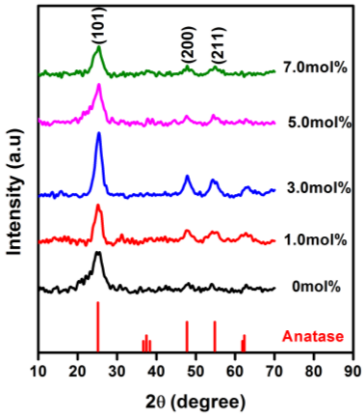

Figure 1. X-ray diffraction patterns for the undoped and Al-doped TiO_2 thin film samples.

The average crystallite size (d) of the samples was estimated using Debye-Scherrer's equation (Kumar *et al.*, 2015; Nadzirah & Hashim, 2013)

$$d = \frac{0.89\lambda}{\beta \cos\theta}$$

where λ the X-ray wavelength of Cu Kα radiation (0.154056nm),θ is the Bragg angle, and β is the experimental full-width half-maximum (FWHM) of the respective diffraction peak (in units of radians). Table 1 show the FWHM and the calculated crystallite size of Al:TiO_2 thin film samples. As reported in Table 1, there is an initial growth in crystallite size from 2.58 nm to 4.20 nm when the doping concentration increased to 3.0 mol% and followed by a size decrease to 3.34 nm as doping reach 7 mol%. The initial crystallite size growth may have contributed by the Al and TiO_2 crystal agglomeration. While for the crystallite size decrement, it may have due to secondary phase growth such as Al_2O_3 which hinder the grain growth and reduction of crystallinity [32], [36].

Table 1. FWHM and crystallite size of Al:TiO_2 thin film samples with different Al doping concentration.

Al Doping (mol%)	2θ	FWHM	Crystallite Size (d) (nm)
0.0	24.82	2.92	2.58
1.0	25.24	2.28	4.15
3.0	25.27	2.31	4.20
5.0	25.41	2.73	3.85
7.0	25.39	2.81	3.34

Figure 2 shows the 3D AFM image of undoped and Al doped TiO_2 thin film samples with different Al doping concentration of Al: 0.0, 1.0, 3.0, 5.0, and 7.0 mol%. From the 2.5μm x 2.5μm scanned 3D AFM images, it is found that microcrystalline structure thin film is successfully grown and all samples are uniformly distributed with hills and valley shaped grains with various sizes. Based on the 3D AFM images, it's clearly seen that the surface morphology of the films change as with doping addition. Thin film with larger size grain is observed as Al doping percentage increased to 7 mol%. The root means square surface roughness (RMS) was further characterized and calculated using Nano navi station Ver. 5.01C software and the data obtain are plot as Figure 3. Figure 3 shows the RMS of Al doped TiO_2 thin film layers deposited with different doping concentration. Based on the figure, the RMS value has initially decreased from 7.07 nm to 1.26 nm as it reach 3 mol% and then increased to 8.54 nm at 7.0 mol% which indicate the surface are becoming more smooth initially and become rougher latter as Al doping concentration increased. It is correlated with the crystallite size data obtained from XRD characterization [37]. Figure 3 displays the crystallite size and RMS of Al:TiO_2 thin film samples with different Al dopant concentration. Based on Figure 3, it shows that the RMS value were decreased (surface roughness become smoother), when the crystallite size increased. According to S. Thanikakarasan *et al.* (2009), larger crystallite size samples have good film stoichiometry, which reduces dislocation density and stacking fault probability, resulting in samples with smoother surfaces and lower RMS [38].

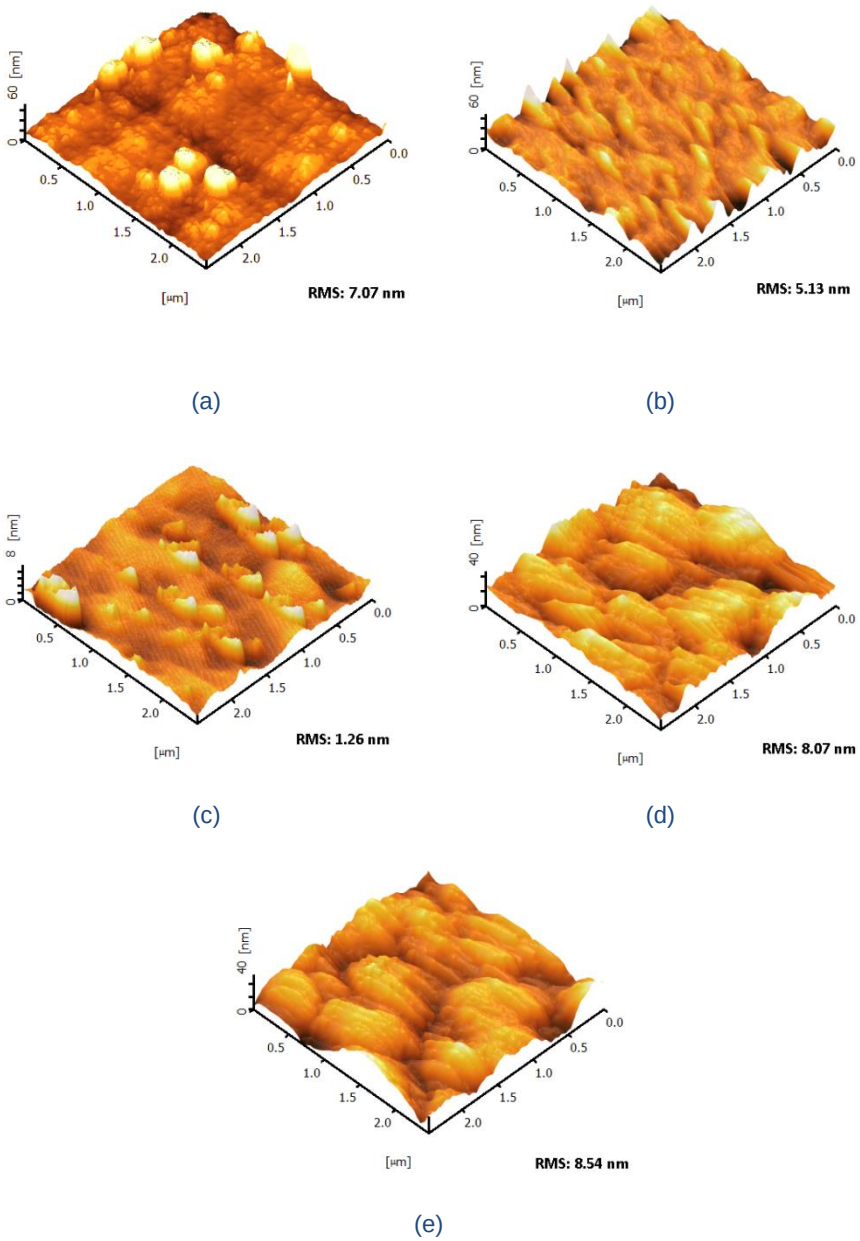

Figure 2. AFM image of all samples:(a) 0 mol% (b) 1 mol% (c) 3 mol% (d) 5 mol% (e) 7 mol%.

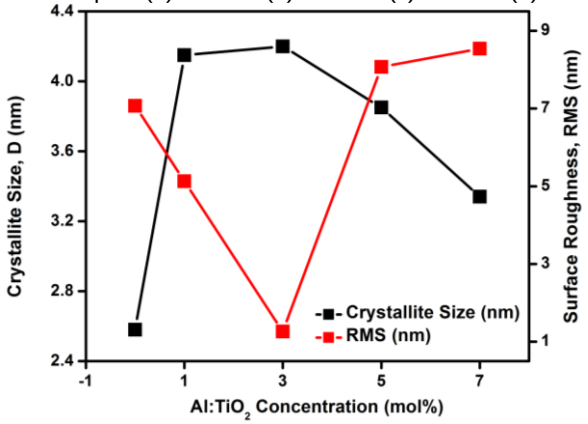

Figure 3. Crystallite size and RMS value for Al:TiO_2 thin film with different doping concentration.

FESEM micrographs of 0.5 mol%, 3mol% and 5.0 mol% Al:TiO_2 thin films are shown in Figure 4 (a), (b) and (c) respectively. It can be clearly seen that the morphology of the all films is uniformly distributed without any crack, but slightly different microstructure. The FESEM image of 0.5 mol% Al:TiO_2 thin film shows lesser and smaller 'white' granular grain compared to 3.0 mol% and 5.0 mol% Al:TiO_2 thin film which showing more and bigger grain. The quantity and size of Al grain are found to increase with the increased of Al doping concentration. The grain quantity and size increment may cause by the coalescence between Al dopant atom with Ti host atom, which reduce the atomic stress and promote the grain growth [36], [39]. To check the homogeneity and identify the elements in the thin film samples, EDX spectra and elemental mapping was carried out. From the EDX spectral and EDX elemental mapping of 5.0 mol% Al:TiO_2 on Figure 4 (c) and (d), show the presence of Ti, O, Al and Si element on the samples and equally distributed over the surface area of the film. The presence of Si is from the glass substrate.

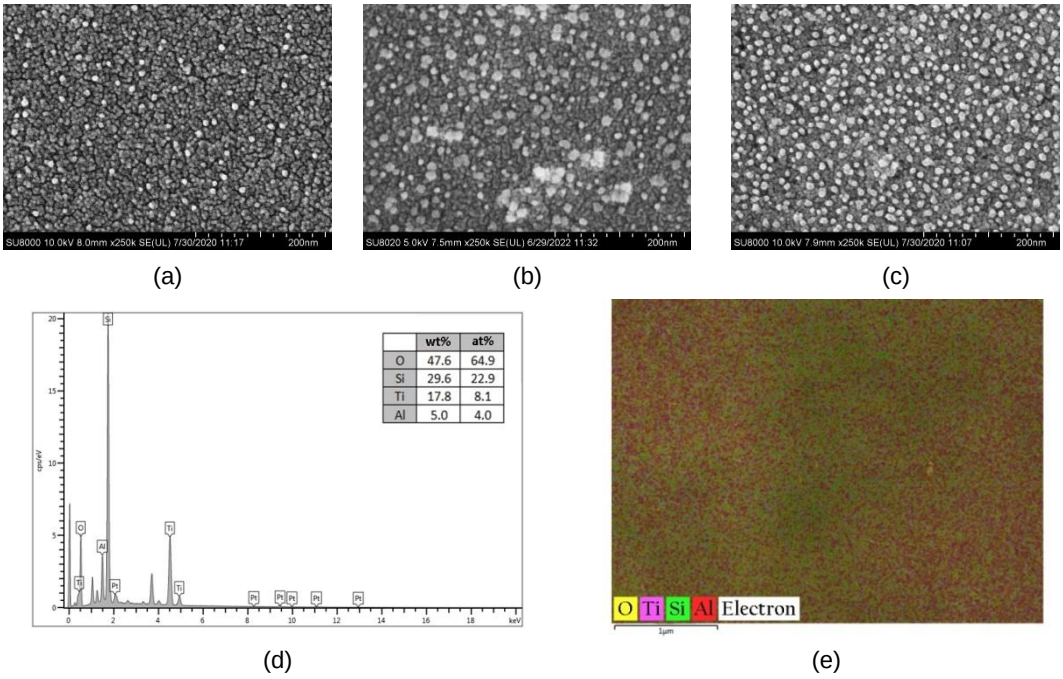

Figure 4. (a) 0.5 mol% sample (x250k magnification)
(b) 3.0 mol% sample (x250k magnification)
(c) 5.0 mol% sample (x250k magnification)
(d) EDX spectra of 5.0 mol% Al:TiO_2.
(e) Elemental mapping of 5.0 mol% Al:TiO_2

Optical Properties

The transmittance spectra for all Al:TiO_2 thin film samples are plotted in Figure 5 and the spectral in range of 300 – 700 nm. Based on Figure 5, it is clearly seen that all thin film samples exhibit high transmittance ranging between 60% and 80% in the visible region (365-680 nm), and it would probably due to relatively low surface roughness, which result in less light scattering [40]. Based on Figure 6, transmittance values has increased with the increased of Al doping and reach highest transmittance for Al:TiO_2 3.0 mol% sample and gradually decreased as the doping percentage increased to Al:TiO_2 7.0 mol%. The decrease of transmittance may due to the increase scattering photon by crystal defect and also may due to free carrier absorption of access doping materials [41]. This suggest that, optical properties of the Al:TiO_2 thin film samples are variable with Al doping concentration.

The optical absorption coefficient (α) can be calculated from the transmittance (T) data and thickness of the film (d), according to the following equation [42]:

$$\propto = \frac{\ln \frac{1}{T}}{d}$$

The energy bandgap (E_g) then was calculated using the well-known Tauc equation [42];

$$\propto = \frac{k(hv - E_g)^n}{hv}$$

where (k) is a constant, (hv) is the photon energy, and the value of n can be $\frac{1}{2}$ or 2 depending on whether it is direct or indirect transitions. The plot of *(αhv)^2 versus (hv)* for all Al:TiO_2 thin film samples is shown in Figure 6. Extrapolating the straight line section of the *(αhv)^2 versus (hv)* graph yields the energy band. Pure TiO2, 1.0 mol% Al:TiO_2, 3.0 mol% Al:TiO_2, 5.0 mol% Al:TiO_2, and 7.0 mol% Al:TiO_2 have estimated energy bandgap values of 4.15 eV, 4.11 eV, 4.10 eV, 4.12 eV, and 4.15 eV, respectively. This is consistent with the XRD data, which indicates crystallite growth and shrinkage [43], [44]. According to the estimated energy band gap, when the doping concentration grew to 3.0 mol%, the energy band gap decreased, perhaps due to the production of energy levels near the TiO_2 valence band by the Al ion. As a result, the energy bandgap between the new modified dopant energy level and the TiO_2 conduction band shrink [45]. Then as the dopant concentration kept increased, the energy band was found increased. Following the Burstein Moss effect, the rise in optical bandgap with increasing Al-dopant concentration may be intrinsically linked to the increase in free-electron concentration caused by the increased of Al doping [8], [40].

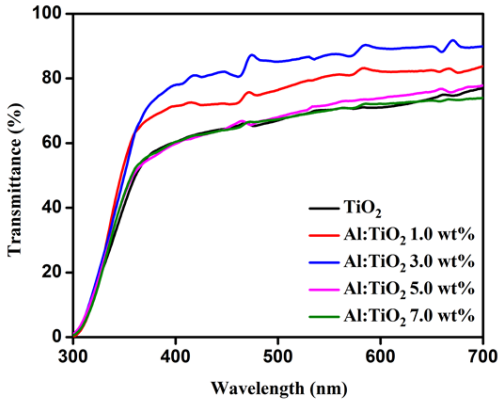

Figure 5. UV-vis transmittance spectra of Al:TiO_2 thin film samples.

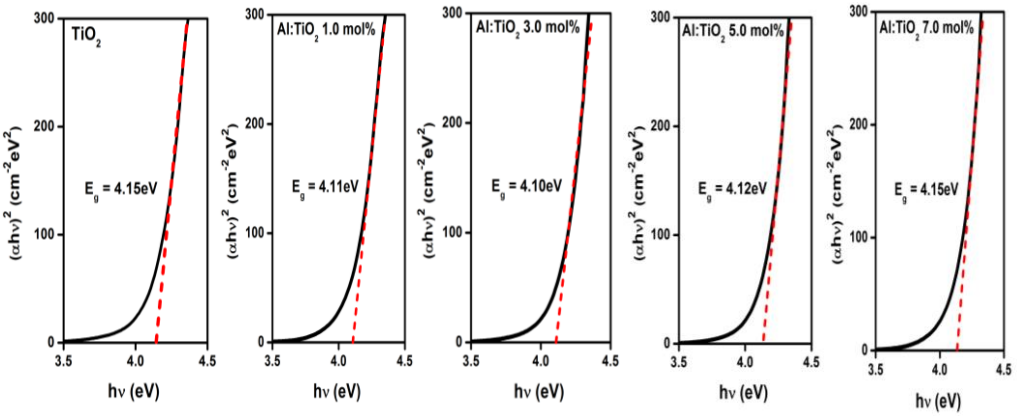

Figure 6. *(αhv)^2 versus (hv)* for all Al:TiO_2 thin film samples.

Conclusions

In summary, Al doped TiO_2 crystalline thin film samples with different Al doping concentration were successfully coated onto glass slide substrate via sol-gel spin coating method. Based on the XRD diffraction pattern, it shown that all thin film samples exhibit anatase phase of TiO_2 with prominent peak of (101) at 2θ = 25.45°. Larger crystallite size and more crystalline structure thin film are observed when

doping concentration reach 3.0 mol%, but decreased as the Al concentration kept increased to 7.0 mol%. AFM image shows, all thin film samples are uniformly distributed with hills and valley shaped grains with various sizes. The RMS was found initially decreased (3 mol%) and then increased as the Al doping concentration kept increased (7 mol%). SEM confirms that doping process has increased the grain size of the Al doped TiO_2 thin film samples. Based on the transmittance spectra, higher transparent Al doped TiO_2 samples are obtain as the doping concentration reach 3.0 mol% but then decreased as the concentration getting higher to 7.0 mol%. Based on the result obtain, the incorporation of Al doping may resulted in changes of the property of TiO_2 thin film and Al doped TiO_2 thin film were more optimum at 3.0 mol% due to the improvement of transmittance of the TiO_2 thin film which can be cooperated to high quality ETL for perovskite solar cell development.

Conflicts of Interest

The author(s) declare(s) that there is no conflict of interest regarding the publication of this paper.

Acknowledgment

This work is part of a research project funded by, FRGS/1/2016/STG07/UTM/02/17, supported by the Ministry of Higher Education, Malaysia, and Universiti Teknologi Malaysia.

References

[1] Hernández-Granados, A., Corpus-Mendoza, A. N., Moreno-Romero, P. M., Rodríguez-Castañeda, C. A., Pascoe-Sussoni, J. E., Castelo-González, O. A., … Hu, H. (2019). Optically uniform thin films of mesoporous TiO2 for perovskite solar cell applications. *Opt. Mater. (Amst).*, *88*(August), 695–703.

[2] S. Nadzirah, K. L. Foo, and U. Hashim. (2015). Morphological reaction on the different stabilizers of titanium dioxide nanoparticles. *Int. J. Electrochem. Sci.*, *10*(7), 5498–5512.

[3] Elfanaoui, A., Elhamri, E., Boulkaddat, L., Ihlal, A., Bouabid, K., Laanab, L., … Portier, X. (2011). Optical and structural properties of TiO_2 thin films prepared by sol-gel spin coating. *Int. J. Hydrogen Energy*, *36*(6), 4130–4133.

[4] M. F. Hossain, S. Naka, and H. Okada. (2018). Annealing effect of E-beam evaporated TiO_2 films and their performance in perovskite solar cells. *J. Photochem. Photobiol. A Chem.*, *360*(February), 109–116.

[5] P. M. Perillo, D. F. Rodríguez, and N. G. Boggio. (2014). TiO_2 nanotubes for room temperature toluene sensor. *OALib*, *01*(07), 1–7.

[6] D. Komaraiah, E. Radha, J. Sivakumar, M. V. Ramana Reddy, and R. Sayanna. (2019). Structural, optical properties and photocatalytic activity of Fe^{3+} doped TiO_2 thin films deposited by sol-gel spin coating. *Surfaces and Interfaces*, *17*(July), 100368.

[7] H. Phattepur, B. S. Gowrishankar, and G. Nagaraju. (2019). Synthesis of gadolinium-doped TiO_2 thin films by sol–gel spin coating technique and its application in degradation of rhodamine-B. *Indian Chem. Eng.*, *61*(2), 167–181.

[8] Bensouici, F., Bououdina, M., Dakhel, A. A., Souier, T., Tala-Ighil, R., Toubane, M., … Cai, W. (2016). Al doping effect on the morphological, structural and photocatalytic properties of TiO_2 thin layers.*Thin Solid Films*. *616*, 655–661.

[9] S. Wu, Z. Weng, X. Liu, K. W. K. Yeung, and P. K. Chu. (2014). Functionalized TiO_2 based nanomaterials for biomedical applications. *Adv. Funct. Mater.*, *24*(35), 5464–5481.

[10] M. Fitra, I. Daut, M. Irwanto, N. Gomesh, and Y. M. Irwan. (2013). TiO_2 dye sensitized solar cells cathode using recycle battery. *Energy Procedia*, *36*, 333–340.

[11] S. N. Sadikin, M. Y. A. Rahman, A. A. Umar, and M. M. Salleh. (2017). Effect of spin-coating cycle on the properties of TiO_2 thin film and performance of DSSC. *12*, 5529–5538.

[12] M. M. Abdoul-Latif, J. Xu, J. X. Yao, and S. Y. Dai. (2017). Au Nanoparticles Doped TiO Mesoporous Perovskite Solar Cells. *Mater. Sci. Forum*.

[13] S. Bhat, K. M. S. Prasad, K. M. Parvathy, and V. S. M. Dharmaprakash. (2019). Effect of Al doping on the carrier transport characteristics of - TiO_2 thin films anchored on glass substrates. *Appl. Phys. A*, *125*(3), 1–11.

[14] G. Liu, X. Wang, Z. Chen, H. M. Cheng, and G. Q. (Max) Lu. (2009). The role of crystal phase in determining photocatalytic activity of nitrogen doped TiO_2. *J. Colloid Interface Sci.*, *329*(2), 331–338.

[15] M. Taylor, R. C. Pullar, I. P. Parkin, and C. Piccirillo. (2020). Nanostructured titanium dioxide coatings prepared by Aerosol Assisted Chemical Vapour Deposition (AACVD). *J. Photochem. Photobiol. A Chem.*, *400*(June),. 112727.

[16] R. Kumar, N. Arorab, and N. Sharmac. (2017). Study of spin coated titanium dioxide films. *Int. J. Pure Appl. Phys.*, *13*(1), 229–231.

[17] D. K. Pallotti, L. Passoni, P. Maddalena, F. Di Fonzo, and S. Lettieri. (2017). Photoluminescence mechanisms in anatase and rutile TiO_2. *J. Phys. Chem. C*, *121*(16), 9011–9021.

[18] Y. M. Sung. (2013). Deposition of TiO_2 blocking layers of photovoltaic cell using rf magnetron sputtering

technology. *Energy Procedia*, *34*, 582–588.

[19] S. Kumar, T. Vats, S. N. Sharma, and J. Kumar. (2018). Investigation of annealing effects on TiO_2 nanotubes synthesized by a hydrothermal method for hybrid solar cells. *Optik (Stuttg).*, *171*(April), 492–500.

[20] M. S. Rahim, M. Z. Sahdan, A. S. Bakri, N. D. M. Said, S. H. A. Yunus, and J. Lias. (2017). Effect of gas on the structural and electrical properties of titanium dioxide film. 030134.

[21] F. I. M. Fazli, N. Nayan, M. K. Ahmad, M. L. M. Napi, N. K. A. Hamed, and N. S. Khalid. (2016). Effect of annealing temperatures on TiO_2 thin films prepared by spray pyrolysis deposition method. *Sains Malaysiana*, *45*(8), 1197–1200.

[22] A. Ranjitha, N. Muthukumarasamy, M. Thambidurai, R. Balasundaraprabhu, and S. Agilan. (2013). Effect of annealing temperature on nanocrystalline TiO_2 thin filmsprepared by sol-gel dip coating method. *Optik (Stuttg).*, *124*(23), 6201–6204.

[23] El Haimeur, A., Makha, M., Bakkali, H., González-Leal, J. M., Blanco, E., Dominguez, M., & Voitenko, Z. V. (2020). Enhanced performance of planar perovskite solar cells using dip-coated TiO_2 as electron transporting layer. *Sol. Energy*, *195*(November 2019), 475–482.

[24] Liu, H., Zhang, Z., Zhang, X., Cai, Y., Zhou, Y., Qin, Q., … Liu, J. M. (2018). Enhanced performance of planar perovskite solar cells using low-temperature processed Ga-doped TiO_2 compact film as efficient electron-transport layer. *Electrochim. Acta*, *272*, 68–76.

[25] G. Yang, H. Tao, P. Qin, W. Ke, and G. Fang. (2016). Recent progress in electron transport layers for efficient perovskite solar cells. *J. Mater. Chem. A*, *4*(11), 3970–3990.

[26] P. Zhao, B. J. Kim, and H. S. Jung. (2018). Passivation in perovskite solar cells: A review. *Mater. Today Energy*, *7*.

[27] N. I. U. Xinshu, L. I. Sujuan, C. H. U. H. ˇH, and Z. Jianguo. (2011). Preparation, characterization of Y 3 + -doped TiO_2 nanoparticles and their photocatalytic activities for methyl orange degradation. *J. Rare Earths*, *29*(3), 225–229.

[28] Zhang, H., Shi, J., Xu, X., Zhu, L., Luo, Y., Li, D., & Meng, Q. (2016). Mg-doped TiO_2 boosts the efficiency of planar perovskite solar cells to exceed 19%. *J. Mater. Chem. A*, *4*(40), 15383–15389.

[29] Duan, Y., Fu, N., Liu, Q., Fang, Y., Zhou, X., Zhang, J., & Lin, Y. (2012). Sn-Doped TiO_2 Photoanode for dye-sensitized solar cells.. 8–13.

[30] S. Bakardjieva and N. Murafa. (2009). Preparation and photocatalytic activity of rare earth doped TiO_2 nanoparticles Václav Stengl. *114*, 217–226.

[31] Pathak, S. K., Abate, A., Ruckdeschel, P., Roose, B., Gödel, K. C., Vaynzof, Y., … Steiner, U. (2014). Performance and stability enhancement of dye-sensitized and perovskite solar cells by al doping of TiO_2. *Adv. Funct. Mater.*, *24*(38), 6046–6055.

[32] Y. S. Song, B. Y. Kim, N. I. Cho, and D. Y. Lee. (2015). Effect of Al doping on optical band gap energy of Al-TiO_2 thin films. *J. Nanosci. Nanotechnol.*, *15*(7), 5228–5231.

[33] Said, N. D. M., Sahdan, M. Z., Ahmad, A., Senain, I., Bakri, A. S., Abdullah, S. A., & Rahim, M. S. (2017). Effects of Al doping on structural, morphology, electrical and optical properties of TiO2 thin film. *030130*, 030130.

[34] S. Nadzirah and U. Hashim. (2013). Annealing effects on titanium dioxide films by Sol-Gel spin coating method. *RSM 2013 IEEE Reg. Symp. Micro Nanoelectron.*. 159–162.

[35] A. Kumar, S. Mondal, S. G. Kumar, and K. S. R. Koteswara Rao. (2015). High performance sol-gel spin-coated titanium dioxide dielectric based MOS structures. *Mater. Sci. Semicond. Process*, *40*, 77–83,

[36] E. M. Mkawi, K. Ibrahim, M. K. M. Ali, M. Farrukh, and S. Mohamed. (2015). The effect of dopant concentration on properties of transparent conducting Al-doped ZnO thin films for efficient Cu_2ZnSnS_4 thin-film solar cells prepared by electrodeposition method. *Appl. Nanosci.*, 993–1001.

[37] D. Gaspar, L. Pereira, K. Gehrke, B. Galler, E. Fortunato, and R. Martins. (2017). High mobility hydrogenated zinc oxide thin films. *Sol. Energy Mater. Sol. Cells*, *163*(June), 255–262.

[38] S. Thanikaikarasan, T. Mahalingam, M. Raja, T. Kim, and Y. D. Kim. (2009). Characterization of electroplated FeSe thin films. *J. Mater. Sci. Mater. Electron.*, *20*(8), 727–734.

[39] S. Majumder, M. Jain, and R. Katiyar. (2002). Investigations on the optical properties of sol–gel derived lanthanum doped lead titanate thin films. *Thin Solid Films*, *402*(1), 90–98.

[40] F. Hanini, Y. Bouachiba, and F. Kermiche. (2013). Characteristics of Al-doped TiO_2 thin films grown by pulsed laser deposition Characteristics of Al-doped TiO_2 thin films grown by pulsed laser deposition. January,.

[41] J. Li, J. Xu, Q. Xu, and G. Fang. (2012). Preparation and characterization of Al doped ZnO thin films by sol-gel process. *J. Alloys Compd.*, *542*, 151–156.

[42] N. R. Mathews, E. R. Morales, M. A. Cortés-Jacome, and J. A. Toledo Antonio. (2009). TiO_2 thin films - Influence of annealing temperature on structural, optical and photocatalytic properties. *Sol. Energy*, *83*(9), 1499–1508.

[43] J. Yu, J. C. Yu, and X. Zhao. (2002). The effect of SiO_2 addition on the grain size and photocatalytic activity of TiO_2 thin films. *J. Sol-Gel Sci. Technol.*, *24*(2), 95–103.

[44] P. Malliga, J. Pandiarajan, N. Prithivikumaran, and K. Neyvasagam. (2014). Influence of film thickness on structural and optical properties of sol – gel spin coated TiO_2 thin film. *IOSR J. Appl. Phys.*, *6*(1), 22–28.

[45] Komaraiah, D., Radha, E., James, J., Kalarikkal, N., Sivakumar, J., Ramana Reddy, M. V., & Sayanna, R. (2019). Effect of particle size and dopant concentration on the Raman and the photoluminescence spectra of TiO_2 :Eu 3+ nanophosphor thin films. *J. Lumin.*, *211*(March), 320–333.